

# Spin-Polaron approach to the Fermi surface evolution in the normal state of cuprates

A. F. Barabanov, R. Hayn<sup>+</sup>, A. A. Kovalev, O. V. J. Razaev, and A. M. Belenouk  
Institute for High Pressure Physics, 142190 Troitsk, Moscow region, Russia

<sup>+</sup> Institute for Solid State and Materials Research (IFW),  
P.O. Box 270016, D-01171 Dresden, Germany

( )

A semi-phenomenological approach to describe the evolution of Fermi surface (FS) and electronic structure with doping is presented which is based on the spin-fermion model. The doping is simulated by a frustration term in the spin Hamiltonian and the complex internal structure of the spin-polaron quasiparticle is taken into account by a superposition of spin-polaron states with different radii. By calculating the spectrum, the spectral weights and the FS we find a rather drastic change of the electronic structure with doping which explains many photoemission data, i.e. the isotropic band bottom and the remnant FS of undoped cuprates, the large FS and the extended saddle point of optimally doped compounds and the pseudogap in the underdoped samples.

PACS number(s): 75.50.Ee, 74.20.Mn, 71.38.+i, 75.30.Mb

## I. INTRODUCTION

The evolution of Fermi surface (FS) and electronic spectrum in the normal state of high temperature superconductors are intensively studied at present. Recent angle-resolved photoemission spectroscopy (ARPES) studies indicate different dispersion relations in the insulating and optimally doped cuprates. The undoped compounds [1,2] show an isotropic band bottom close to  $N = (\pi/2; \pi/2)$  in momentum space, a large energy difference between  $N$  and  $X = (\pi; 0)$ , and a so-called remnant Fermi surface [3] (that surface where the single particle spectral weight shows a sudden drop of intensity). In the optimally doped compounds a flat band region, a large FS centered at  $M = (\pi; \pi)$  and a so-called shadow Fermi surface due to antiferromagnetic (AFM) spin correlations [4] are found [5-11]. The flat band region has the form of an extended saddle point which stretches in the direction  $(\pi/2; 0) - (\pi; 0)$ . The shadow FS resembles the main FS but is shifted by the AFM vector  $Q = (\pi; \pi)$ . Furthermore, the underdoped compounds demonstrate the existence of a high energy pseudogap near the point  $X$  with an energy of about 0.1–0.2 eV [2,12-14]. Assuming a simple rigid band filling, the isotropic minimum of the undoped compounds would suggest small hole pockets around  $N$ . However, there are no clear experimental indications for them [14] and the Fermi surface seems to develop in an arc-like fashion [15]. It is a real theoretical problem to reconcile that seeming contradiction which can be attacked only by considering the spectral density evolution as a whole.

There are numerous studies of the hole spectrum in two dimensional (2D) doped antiferromagnets using a wealth of theoretical models, like the generalized t-J, the effective three-band model, the Kondo-lattice or the Hubbard model. Most of those studies are restricted to a very low hole concentration using the exact diagonalization of small clusters [16,17], the quantum Monte Carlo technique [18], the self-consistent Born approximation (SCBA) [19-21] or a "string" ansatz for the hole wave function [22]. One can start either from the two-sublattice Neel-type state [19,20,22,23] or from the spin rotationally invariant spin liquid state [35,34] and obtain qualitatively the same result: the hole motion takes place mainly on one sublattice, i.e. the dispersion relation is dominated by an effective hopping to the next nearest neighbors and the dispersion has its minimum at  $\Gamma$  for small doping. There are much less attempts to explain the Fermi surface evolution, like for instance [24] which used a diagrammatic method combined with a semi-phenomenological spin susceptibility. The exact diagonalization studies (on clusters containing up to  $16 \times 20$  sites) at finite hole doping [25-27] have difficulties to reconstruct the FS and to investigate a sufficiently smooth variation of doping due to the restricted set of  $k$ -points.

The approach which shall be presented here is semi-phenomenological as well. On one hand, we start with the spin-fermion model (the reduced form of the three-band Emery model) that has a clear microscopic basis [28,29]. We also include direct oxygen-oxygen hopping terms which are rather important. On the other hand, we simulate the doping by a frustration term  $J_2$  in addition to the nearest neighbor exchange  $J_1$  of the spin part in the Hamiltonian. The similarity between doping and frustration had been first proposed in [30] based on a similar decrease of the magnetic correlation length. It is interesting to note that cluster calculations indicated a considerable value of the frustration parameter  $J_2/J_1 \approx 0.1$  even for the undoped  $\text{La}_2\text{CuO}_4$  [31]. Of course there is no full equivalence between doping and frustration. For example, the doped t-J model and the frustrated  $J_1$ - $J_2$  model give different results for the dynamical spin-spin structure factor and for the spectrum of Raman scattering [32]. But numerical calculations on finite lattices indicate the equivalence of the mentioned models if we are interested in the static spin-spin correlation functions [33]. And those quantities are especially relevant in our present Green's function method where the spectrum  $\chi''(\mathbf{k})$  is determined by the static spin-spin correlation functions of the spin subsystem.

Previous studies of the frustrated generalized t-J [34] and the frustrated effective three-band model [35] demonstrated already the strong influence of frustration on the spin-polaron spectrum. However, these investigations were performed only within the local polaron approach (LPA) which cannot describe the influence of long range spin order on the excitation spectrum. Furthermore, only the bare spectral weight was considered which could only give a hypothetical FS. Recently [36] the frustrated t- $t'$ - $t''$ - $J_1$ - $J_2$  model was discussed in the framework of the SCBA where the holes are treated as spinless fermions and the spins as normal bosons [20]. The resulting SCBA in [36] corresponds to a two sublattice approach in which the spectrum is dictated by the symmetry of the reduced magnetic Brillouin zone (BZ) (e.g. the points  $\Gamma$  and  $M$  are equivalent). However, such a symmetry is not reproduced in the ARPES data. On the contrary, the spherically symmetric approach (in the spin space) is used in the present investigation to describe the spin subsystem. As a result, the spectrum is periodic relative to the full Brillouin

zone (BZ) of the  $\text{CuO}_2$  plane.

The distinctive feature of our present investigation consists in treating the spin-polaron as a complex quasiparticle, i.e. as a superposition of spin polaron states with different radii [37]. Our basis operators enclose the local polaron (bare holes and the Zhang-Rice polaron) and also its coupling to spin waves with quasimomentum  $q$  close to the antiferromagnetic wave vector  $Q$ . By introducing the complex structure of the spin-polaron one may describe the important splitting of the lowest local polaron band. This allows, for example, to reproduce for heavily underdoped compounds a sudden drop in the intensity of ARPES peaks as  $k$  goes from  $N$  to  $M$ . And we will show that it reproduces also many of the other features of electronic structure evolution mentioned above.

## II. THE HAMILTONIAN AND THE METHOD

The main features of the hole motion in the  $\text{CuO}_2$  plane are described by the model [28,29]:

$$\hat{H} = \hat{H}_0 + \hat{J} + \hat{h}; \quad (1)$$

$$\hat{H}_0 = 4 \sum_R \mathbf{p}_R^y \frac{1}{2} + \mathbf{S}_R \cdot \mathbf{p}_R; \quad (2)$$

$$\hat{J} = \frac{J_1}{2} \sum_{R, g} \mathbf{S}_R \cdot \mathbf{S}_{R+g} + \frac{J_2}{2} \sum_{R, d} \mathbf{S}_R \cdot \mathbf{S}_{R+d} \quad (3)$$

where  $J_1, J_2 > 0$  are the antiferromagnetic interactions between the first-nearest neighbor ( $g = \mathbf{g}_x; \mathbf{g}_y$ ) and the second-nearest neighbor ( $d = \mathbf{g}_x, \mathbf{g}_y$ ) on a square lattice. The direct oxygen-oxygen hopping is included by

$$\hat{h} = \sum_R \sum_{\mathbf{a}} c_{R+\mathbf{a}}^y c_{R+\mathbf{a}_y} + c_{R-\mathbf{a}_y} c_{R+\mathbf{a}_y} + c_{R+\mathbf{g}_x+\mathbf{a}_y} c_{R+\mathbf{g}_x-\mathbf{a}_y} + \text{h.c.}; \quad (4)$$

with

$$\mathbf{p}_R = \frac{1}{2} \sum_{\mathbf{a}} c_{R+\mathbf{a}}; \quad \mathbf{S}_R = \frac{1}{2} \sum_{\mathbf{a}} c_{R+\mathbf{a}}^\dagger \boldsymbol{\sigma} c_{R+\mathbf{a}}; \quad \mathbf{p}_R^y; \mathbf{p}_R^0 = \frac{1}{4} \sum_{\mathbf{g}} c_{R+\mathbf{g}}^\dagger c_{R+\mathbf{g}}; \quad (5)$$

where  $\mathbf{a}_{xy} = \frac{1}{2} \mathbf{g}_{xy}$ :

Here and below the summation over repeated indexes is understood everywhere;  $[\dots]; [\dots]$  stand for anticommutator and commutator respectively;  $\mathbf{g}_{xy}$  are basis vectors of a copper square lattice ( $|\mathbf{g}| = 1$ ),  $R + \mathbf{a}$  are four vectors of O sites nearest to the Cu site  $R$ ; the operator  $c_{R+\mathbf{a}}^y$  creates a hole predominantly at the O site (the spin index is dropped in order to simplify the notations);  $\boldsymbol{\sigma}$  are the Pauli matrices; the operator  $\mathbf{S}$  represents the localized spin on the copper site. We do not introduce the explicit relative

phases of p- and d-orbitals since they can be transformed out by redefining the operators with phase factors  $\exp(iQ \cdot R)$ . In order to compare our results with other authors and with experiment we restore these phases by changing in the final results  $k \rightarrow k - Q$ . The parameter  $t$  is the hopping amplitude of oxygen holes that takes into account the coupling of the hole motion with the copper spin subsystem. For convenience, the exchange interactions  $J_1$  and  $J_2$  can be expressed in terms of the frustration parameter  $p$ :

$$J_1 = (1 - p)J; \quad J_2 = pJ; \quad 0 \leq p \leq 1; \quad J > 0: \quad (6)$$

The frustration parameter  $p$  has to be connected with the number  $x$  of holes per copper atom. We are guided by an estimate based on the single-band Hubbard model with realistic values of  $U \approx 5$  for  $x = 0.1$  where one finds a value of  $p \approx 0.1$ . Let us note that in the case of  $\text{La}_{2-x}\text{Sr}_x\text{CuO}_4$  the spin system of the  $\text{CuO}_2$  plane loses its long-range order for  $x > 0.02$ .

The adopted effective spin-fermion Hamiltonian can be obtained by canonical transformation from the Emery model [38] in the regime  $U_d \gg t, \mu = \mu_p = \mu_d > 0$ , where  $U_d$  is the Coulomb repulsion on copper sites. The values of the energy parameter set  $\mu, t, U_d$  may be extracted from band structure or cluster calculations. Two typical sets are:  $\mu = \mu_p = \mu_d = 3.6 \text{ eV}, t = 1.3 \text{ eV}, U_d = 10.5 \text{ eV}$ , [39], or  $\mu = 2.0 \text{ eV}, t = 1.0 \text{ eV}, U_d = 8.0 \text{ eV}$  [40,41]. Taking into account that  $t = \mu, J \approx 4(t = \mu)^2$  we adopt the parameter values  $t = 0.4 \text{ eV}, J = 0.4$  and  $\hbar = 0.4$ . Below we take as the unit of energy. We consider a spin-liquid state with spin rotational symmetry for the copper subsystem, e.g. the spin-spin correlation functions satisfy the relation  $C_r = S_r S_{r+r} = 3 S_r^{x(y;z)} S_{r+r}^{x(y;z)}; \quad \langle S_r \rangle = 0$ :

To treat the problem of a spin-polaron in the projection method approach we introduce a finite set of basis operators connected with each cell  $R: A_{R,ji}^+$  (with spin  $i$ ), where  $i$  is the number of the operator,  $i = 1 \dots N$ . The set contains the creation of a hole (with spin  $i$ ) and other operators which describe a hole connected with spin excitations at different distances. The choice of the set is dictated by the physical sense of the problem and will be explained in detail below. To calculate the spectral function of bare holes we take the sum of two contributions  $c_{R+a_x}^+$  and  $c_{R+a_y}^+$  that are related with two possible positions of an oxygen hole in the unit cell.

As usual we introduce the retarded two-time Green's functions  $G_{ij}(t; k)$  defined in terms of the Fourier transforms  $A_{k,ji}$  of the operators  $A_{R,ji}$ :

$$G_{ij}(t; k) = \frac{D}{N} \sum_R A_{k,ji}(t) \tilde{A}_{k,jj}^+(0) = \frac{E}{N} \sum_R A_{k,ji}(t) A_{k,jj}^+(0); \quad (7)$$

$$A_{k,jj} = \frac{1}{N} \sum_R e^{ikR} A_{R,jj}; \quad i, j = 1 \dots N:$$

The equations of motion for the Fourier transforms of the Green's functions have the form

$$\begin{aligned} \frac{D}{N} \sum_R A_{k,ji}(t) \tilde{A}_{k,jj}^+(0) &= K_{ij} + \frac{E}{N} \sum_R B_{k,ji} \tilde{A}_{k,jj}^+(0) \\ K_{ij}(k) &= A_{k,ji} A_{k,jj}^+; \quad B_{k,ji} = A_{k,ji} H; \end{aligned} \quad (8)$$

In the projection technique we approximate the new operators  $B_{k,i}$  by their projections on the space  $\{A_{k,i}\}$  of the basis operators:

$$B_{k,i} = \sum_{j=1}^N L_{ij}(k) A_{k,j}; \quad L(k) = D(k) K^{-1}; \quad D_{ij}(k) = \langle B_{k,i} | A_{k,j}^\dagger \rangle; \quad (9)$$

After substitution of the approximate expressions for the operators  $B_{k,i}$  in (9) into the equations of motion (8), the equation system (8) for Green's functions  $A_{k,i} A_{k,j}^\dagger$  becomes closed and can be presented in the matrix form

$$(E - D K^{-1}) G = K; \quad (10)$$

where  $E$  is the unit matrix. The quasiparticle spectrum  $\epsilon(k)$  is determined by the poles of the Green's function  $G$  and can be derived from the condition

$$\det K^{-1}(k) = 0;$$

### III. THE BASIS OPERATORS AND APPROXIMATIONS

At first we choose a set of three basis operators which describe local spin-polaron states

$$A_{R,1} = \frac{1}{2} (C_R + a_x + C_R a_x); \quad A_{R,2} = \frac{1}{2} (C_R + a_y + C_R a_y); \quad A_{R,3} = S_R P_R; \quad (11)$$

The combinations of them constitute the Zhang-Rice polaron and bare hole states, in particular:

$$C_{k,x} = \frac{2}{1 + \exp(ik_x)} A_{k,1}; \quad C_{k,y} = \frac{2}{1 + \exp(ik_y)} A_{k,2}; \quad C_{k,x(y)} = \frac{1}{N} \sum_R e^{ikR} C_{R+a_{x(y)}}; \quad (12)$$

The spectrum of elementary excitations in the framework of the local polaron approach (LPA) was investigated previously [35]. In particular it was pointed out that the frustration in spin subsystem and oxygen-oxygen hopping can explain the appearance of an extended saddle-point in the spectrum. The main shortcoming of LPA consists in the fact that the spectrum of elementary excitations depends only on the short range spin-spin correlation functions even at zero temperature. This means that LPA does not describe the influence of spin long range order on the excitation spectrum.

Treating the periodic Kondo problem on a square lattice in the two sublattice spin structure, Schrieffer [42] emphasized the crucial importance of taking into account coherence factors related to the existence of long range order. In this model the band electrons (holes) are coupled to localized spins and the simplest Hamiltonian has the form

$$H_K = \sum_{R \neq g} t_g c_{R+g}^\dagger c_R + I \sum_R c_R^\dagger S_R c_R + \frac{1}{2} J \sum_{R \neq g} S_{R+g} S_R \quad (13)$$

where the onsite exchange with constant  $I$  is analogous to the  $\hat{H}$  Hamiltonian (2) in our model. In Ref. [42] the mean-field approach was taken for the Neel state at  $T = 0$  and the spins were treated as classical vectors:

$$S_R = S_0 e^{iQ \cdot R}; \quad S_0 = \text{const.} \quad (14)$$

In this approximation the Kondo-interaction Hamiltonian (13) takes the form of a potential energy with doubled period. As a result, this interaction leads to the hybridization of bare particle states with momenta  $k$  and  $k + Q$  and one should perform a standard unitary transformation to take into account this hybridization from the very beginning. In the adopted Neel state the amplitude  $S_Q$  of the spin wave with  $q = Q$  (the  $Q$ -wave) has a macroscopic large value and has properties analogous to the amplitude of a Bose particle with zero momentum in the superfluid Bose-gas. As a result, this amplitude can be treated as a c-number for many problems. Then the hybridization corresponds to coupling of the  $Q$ -wave to local electron states. But it does not represent new states and leads only to mixing of states with momenta  $k$  and  $k + Q$ .

The distinctive feature of the present investigation consists in considering the one-particle motion on the background of the spherically symmetric spin subsystem state. In this background the average value  $\langle S_Q \rangle = 0$  and the above mentioned treatment fails. At  $T = 0$  and without frustration the only value which can be treated as a macroscopic one is  $\langle S_Q S_Q \rangle$ . Then the coupling of a local state to  $S_Q$  corresponds to a new delocalized spin polaron states { local polaron states (11) dressed by antiferromagnetic spin wave  $S_Q$ . For the model under discussion at  $T = 0$  such states were introduced in [43] and have the form

$$Q_i A_{R,ji}; \quad i = 1; 2; 3 \quad (15)$$

$$Q_R = e^{iQ \cdot R} S_Q; \quad S_Q = S_Q^\dagger; \quad S_Q = N^{-1} \sum_{R_1} e^{iQ \cdot R_1} S_{R_1}; \quad (16)$$

It was shown in [43] that it is important to take into account the quantum nature of the spin  $Q$ -wave because the transitions between the local polaron states and the delocalized polaron states lead to a splitting of the lowest LPA bands and change their properties in an essential way. Only the complex spin-polaron approach, i.e. that approach containing the local spin-polaron operators plus those operators dressed by the  $Q$ -wave, can be compared with a Green's function calculation for the bare hole spectral function  $A_h(k; !)$  taking into account the spin-polaron damping by means of the SCBA [44]. One can see that the SCBA quasiparticle peak and its intensity are well given by the lowest band of the complex spin-polaron approach, whereas the excited bands reflect the non-coherent part of  $A_h(k; !)$ .

In the present paper we treat the model at nonzero temperatures  $T$  and frustration  $p$ . In this case, the spin subsystem loses its long-range order and the average value

$\langle S_Q S_Q \rangle$  is zero. So one must introduce new operators in order to preserve the complex spin-polaron results and to take into account a finite spin correlation length. It is natural to generalize the above choice of operators by introducing local polaron states dressed by spin waves with momenta  $q$  close to the antiferromagnetic vector  $Q$  (for such  $q$  the spin-spin structure factor is sharply peaked even at  $T; p \neq 0$ ). These operators can be taken in the form:

$$A_{R;4} = Q_R^{(\cdot)} A_{R;1}; \quad A_{R;5} = Q_R^{(\cdot)} A_{R;2}; \quad A_{R;6} = Q_R^{(\cdot)} A_{R;3} \quad (17)$$

$$Q_R^{(\cdot)} = N^{-1} \sum_{q \in \Omega} e^{iq \cdot R} S_{R+q}; \quad \Omega = \{q; j \in \Omega_j, q_j < \pi\} \quad (18)$$

Here  $\Omega$  is the square region around  $Q$  and around equivalent points (described by the four squares  $\Omega_j = \Omega_j + Q$  related to the corners of the first Brillouin zone (BZ), see Fig. 1.1a). The choice of the parameter  $\pi$  is dictated by the spin correlation length which depends on the frustration. In order to clarify our future choice of the parameter  $\pi$  for different frustrations let us represent each of the operators in (17) (taking  $A_{R;4}$  as an example) in the form

$$A_{R;4} = \sum_{R^0} (R - R^0) e^{iQ \cdot (R - R^0)} S_{R^0} A_{R^0;1} \quad (19)$$

where

$$(l) = \int_{\Omega} \frac{d^2 k}{(2\pi)^2} e^{ik \cdot l} \quad (20)$$

The absolute value of  $(R - R^0)$  depends only on the absolute value of the difference  $l = R - R^0$  and decreases with the increase of  $l$ . This dependence  $\sim(l) = j(l) = (0)j$  has the form

$$\sim(l) = j \sin(l_x / l_0) \sin(l_y / l_0) = (l_x l_y / l_0^2) j \quad (21)$$

The value  $l_0$ , which satisfies the condition

$$l_0 = \pi; \quad (22)$$

can be qualitatively treated as a coupling radius of the local polaron which defines the range of coupling to the long distance spin correlations, since  $\sim(l) \approx 1$  for  $l < l_0$  and  $\sim(l) \approx 0$  for  $l > l_0$ . On the other hand, the coupling radius of a spin polaron must be of the order of the spin correlation length  $l_0$ . This qualitative estimation leads to the choice  $l_0 = \pi^2 / 2; \quad \pi_0 = \pi$ . Such a choice of  $\pi$  gives a correct description of two limits. If  $\pi$  tends to infinity (the spin system has long range order,  $T = 0$ ), the coupling radius of polaron also tends to infinity,  $l_0$  tends to zero and  $Q_R^{(\cdot)}$  (18) is transformed to  $Q_R$  from (16). It is clear that in the opposite limit of high temperature, when the spin correlation between neighboring sites is small, the system must be described by local spin polarons.

As it is seen from (22) if  $(\frac{1}{2})$  tends to unity the value  $\rho_0$  is close to 1. In this case  $(R \cdot R^0) = R \cdot R^0$  and the operators  $A_{R,i}; i = 4;5;6$  represent local spin polarons close to polarons  $A_{R,i}; i = 1;2;3$  (in particular, for  $\rho_0 = 1$ ,  $A_{R,6}$  is the linear combination of  $A_{R,1}$ ,  $A_{R,2}$ , and  $A_{R,3}$ ). As a result, we have a continuous description of the model from finite temperature to zero one.

The spin correlation length was determined taking the spin wave spectrum which was calculated for the frustrated Heisenberg model in the framework of the spherically symmetric approach [45]. If the spin system is not far from the Neel phase,  $\rho_0$  may be determined using the expansion of the spectrum close to the AFM point  $Q$  [46], which will be denoted by  $Q_0$ . Then we use the criterion  $\rho_0 = \rho_{Q_0}$ : The explicit expressions of spectrum and  $Q_0$  are given in Appendix A. The choice of the parameter  $\rho_0$  is different when  $Q_0$  becomes small. The value of  $Q_0$  depends strongly on the frustration parameter  $p$ . For  $p = 0.15$  we have  $Q_0 = 2.3$  ( $\rho_0 = \rho_{Q_0} = 0.35$ ) and for such a frustration the real value of  $\rho_0$  can essentially differ from  $Q_0$ . Indeed, for the frustrated case the spin-spin correlation functions  $C_R = \langle S_{R_0} S_{R_0+R} \rangle$  have the following dependence on  $R = n_x g_x + n_y g_y$ :

$$C_R = m_1(R) (\frac{1}{2})^{n_x + n_y} + m_2(R) [(\frac{1}{2})^{n_x} + (\frac{1}{2})^{n_y}] \quad (23)$$

where  $m_1(R) = m_2(R)$  for  $p = 1$  (Neel type phase) and  $m_1(R) \neq m_2(R)$  for  $p$  close to unity (stripe phase with gapless spectrum at points  $Q_1 = (\frac{1}{2}; 0); (0; \frac{1}{2})$ ). The values  $m_1(R)$  and  $m_2(R)$  are dictated by the spin spectrum gaps in the points  $Q$  and  $Q_1$ : For intermediate values of frustration  $0.15 < p < 0.55$  these gaps of the spin spectrum are comparable, and in this  $p$ -interval it is meaningless to determine  $\rho_0$  by the expansion of the spectrum near the points  $Q$  or  $Q_1$ . On the other hand, a local polaron structure is taken into account by the operators  $A_{R,1}$ ,  $A_{R,2}$ ,  $A_{R,3}$  and the operators  $A_{R,4}$ ,  $A_{R,5}$ ,  $A_{R,6}$  are introduced as candidates to describe polaron states with large or intermediate radius  $l_0 = 2.3$ . This means that we should  $x_0' = 0.35$  for  $p = 0.15$  ( $\rho_0 = \rho_{l_0}$ ;  $l_0 = 2.3$ ) and take  $\rho_0 = \rho_{Q_0}$  for  $p < 0.15$ . The calculated values of  $Q_0$  and the adopted below relation between the values of the parameter  $\rho_0$  and different frustrations are represented in Table 1.

To find the spectrum of excitations in the framework of the operators (11), (17) we calculate the matrix elements for matrices  $D$  and  $K$ . The calculation of elements of the arrays  $D$  and  $K$  is usually lengthy and it involves the calculation of complex commutators for the operators  $A_{k,i}$  and  $B_{k,i}$ . Some of these commutators cannot be expressed explicitly by two-site Green's functions and some approximations are needed. The matrix elements are considerably simplified for a one-hole approach which can be adopted due to treating the problem in the limit of low doping (we will consider doping  $n < 0.2$ ). Then they are expressed in terms of two- and multi-site correlation functions of spin operators (in the cases considered below — two-, three-, four- and five-site correlation functions). By taking into account the spherical symmetry the three-site correlators can be reduced to two-site correlators, and five-site correlators can be reduced to four-site correlators. The four-site correlators can be reduced to the form

$$V_{R_1 R_2 R_3 R_4} = h(S_{R_1} S_{R_2}) (S_{R_3} S_{R_4}) i;$$



where all sites are supposed to be different. To calculate such correlators an approximation [47] is used:

$$V_{R_1 R_2 R_3 R_4} = C_{R_{12}} C_{R_{34}} + \frac{1}{3} C_{R_{13}} C_{R_{24}} + \frac{1}{3} C_{R_{14}} C_{R_{23}} :$$

As a result the matrix elements are expressed over the static spin-spin structure factor  $C_q$  (Fourier transform of  $C_R$ ). The explicit form of  $K$  and  $D$  matrix elements are reproduced in Appendix B. Typical sums in the matrix elements have the form :

$$u_g = N^{-1} \sum_{q_2} e^{iq_g} C_q; \quad W_{g1}^{(J)} = N^{-2} \sum_{q_1, q_2} e^{iq_2 g} C_{q_1 - q_2} C_{q_2} : \quad (24)$$

The expressions analogous to  $u_g$  and  $W_{g1}^{(J)}$  contain one and two summations on  $q_2$ . Each sum on  $q$  is proportional to  $\omega^{-2}$  which is a small parameter in our approximation: as mentioned above  $\omega^{-2} = \frac{2}{\omega_0^2} \approx 0.1$  (see Table 1). This smallness allows to justify the approximation which consists in neglecting some terms proportional to  $\omega^{-2}$ .

#### IV . R E S U L T S A N D D I S C U S S I O N

After solving the system (10) for the chosen set of operators  $A_{R,ji}$  the resulting Green's functions have the form

$$G_{ij}(\omega; k) = \sum_{l=1}^6 \frac{z_{(ij)}^{(l)}(k)}{\omega_l(k)}; \quad i, j = 1 \dots 6 : \quad (25)$$

According to (12) the residues  $z_{(1,1)}^{(l)}(k)$ ,  $z_{(2,2)}^{(l)}(k)$  determine the spectral weights  $n_{h,i}^{(l)}(k)$  of bare oxygen holes with fixed spin and momentum  $k$  in the quasiparticle state  $|k; i\rangle$  of the quasiparticle band  $\omega_l(k)$ :

$$n_{h,i}^{(l)}(k) = \frac{2}{1 + \cos(k_x)} z_{(1,1)}^{(l)}(k) + \frac{2}{1 + \cos(k_y)} z_{(2,2)}^{(l)}(k) : \quad (26)$$

Let us remind that the bare hole spectral weight satisfies the sum rule  $\sum_l n_{h,i}^{(l)}(k) = 2$  and the maximum number of holes per cell is equal to four despite the presence of six bands. This means that in this model the Luttinger theorem is not fulfilled.

We present the results of the spin-polaron spectrum calculation for a temperature  $T = 0.2J$ . Let us mention that the spectrum has a weak temperature dependence up to a temperature  $T = 0.4J$ . Since we are interested in relatively small doping values  $x = 0.2$  we represent results for the two lowest bands  $l = 1, 2$  only. In the high doping regime our approach may be insufficient since it is based on the one hole approximation and does not take into account the interaction between polarons.

In Fig. 1 the spectrum  $\omega_l(k)$  and the bare hole spectral weight  $n_{h,i}^{(l)}(k)$  of the lowest band for different values of the frustration parameter,  $p = 0.05, 0.1, 0.13, 0.15, 0.2$  and

0.25, are presented by contour plots taking  $\hbar^2$  as the unit of energy. As mentioned already, we suppose some qualitative equivalence between doping  $x$  and frustration  $p$ .

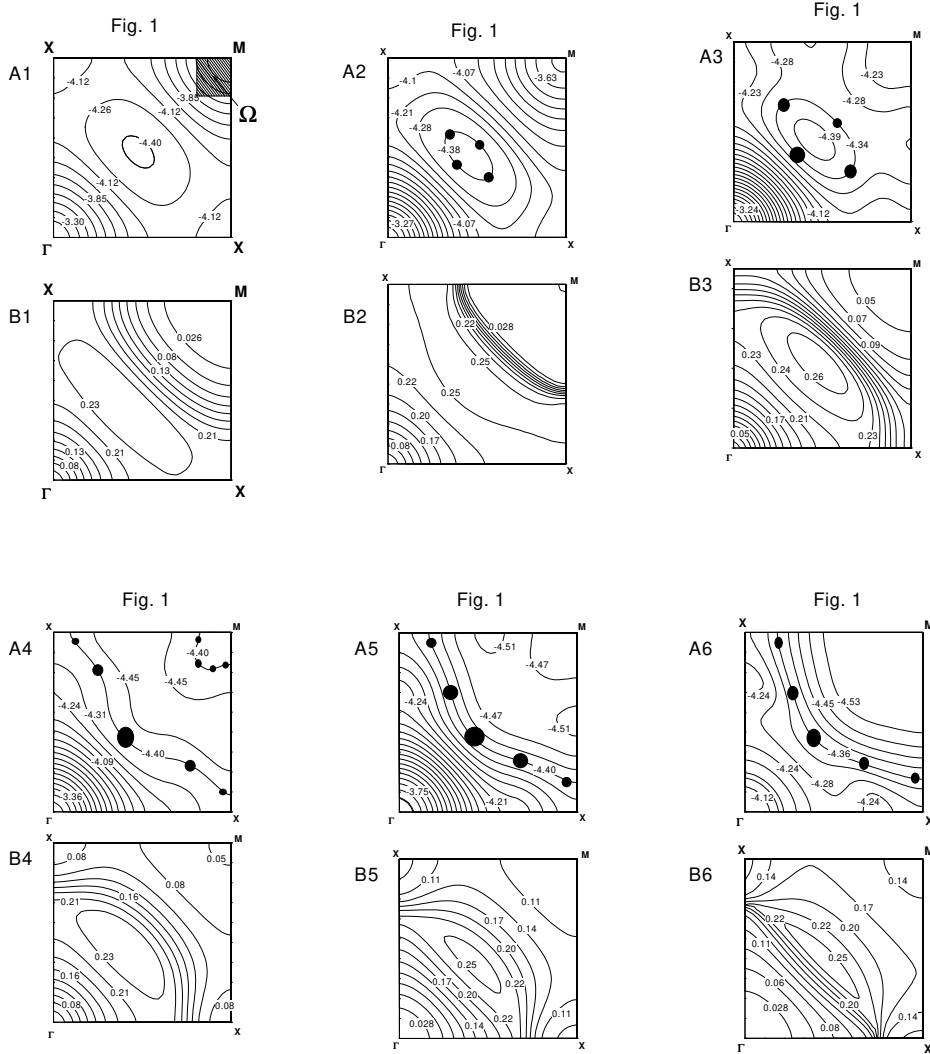


Fig.1: Spectrum  $\epsilon_1(k)$  (figures a) and bare hole spectral weight  $n_{h,i}^{(1)}(k)$  (figures b) for the lowest band presented as contour plots (in units  $\hbar^2 = 1$ ) for different values of the frustration parameter  $p$  (0.05, 0.10, 0.13, 0.15, 0.20 and 0.25) corresponding to Figs. 1:1 – 1:6. The symmetry points in the first quadrant of the BZ are denoted as  $\Gamma = (0;0)$ ;  $X = (\pi;0)$ ;  $M = (\pi;\pi)$ .

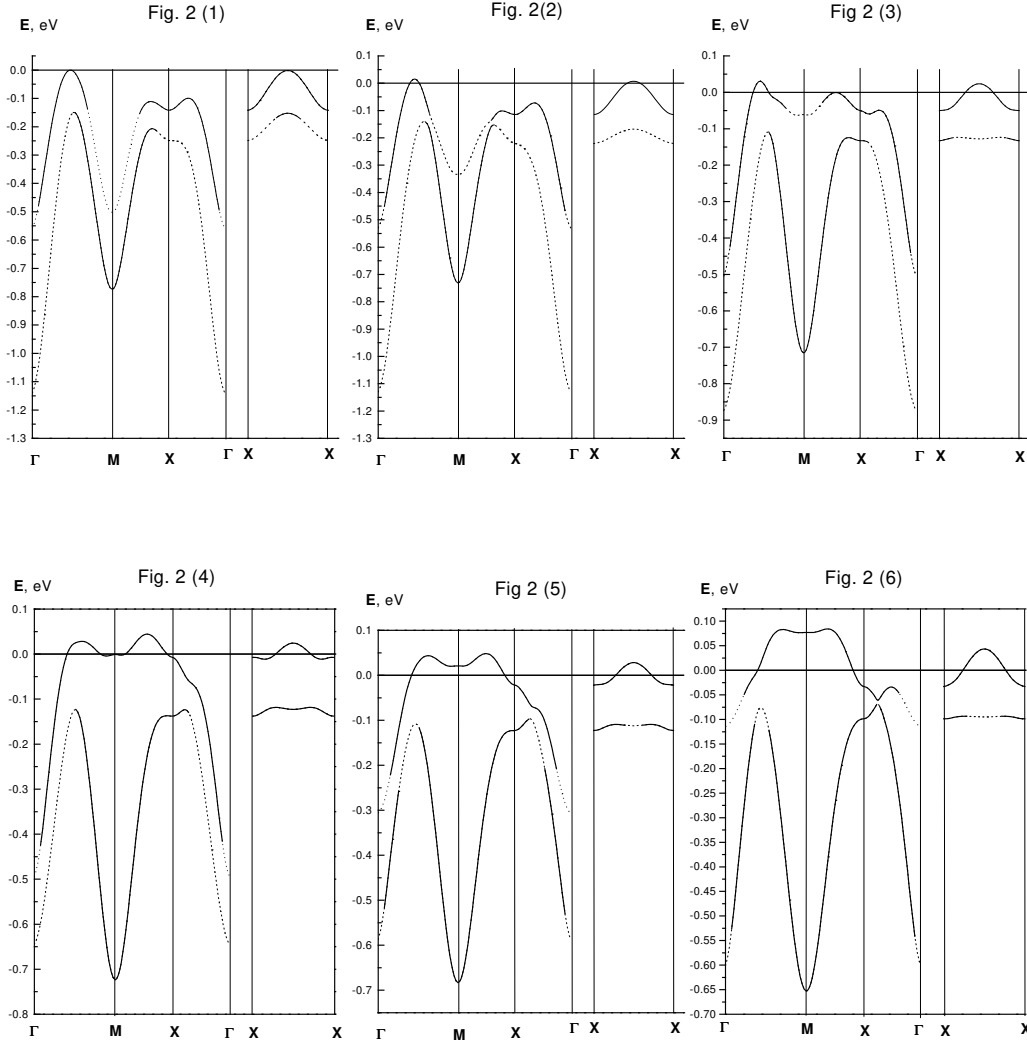


Fig 2: Electronic spectrum of the two lowest hole bands for the same frustration parameters as in Fig. 1 along high symmetry lines of the BZ. Zero energy corresponds to the Fermi level and the value of  $t$  has been set to 0.4 eV. The parts of both bands which have considerable spectral weight  $n_h^{(1,2)}(k) > 0.05$  are plotted by solid lines, the parts with small weight by dotted lines.

The relation adopted below  $x$ ,  $p$  is given in Table 1. Of course this relation is a phenomenological one and it may need some rescaling. Nevertheless, the main conclusions are preserved if we admit the realistic assumption that the small and optimal dopings

correspond to  $p = 0.1$  and  $p = 0.125$ , accordingly. The contours decorated by full circles correspond to the Fermi surfaces calculated for the hole dopings  $x$  from Table 1. The diameter of the circles is proportional to the spectral weight  $n_{h,i}^{(1)}(k)$  along the FS. In Fig. 2 we show the electronic spectrum for the two lowest bands along high symmetry lines for the value of  $\epsilon = 0.4$  eV as adopted in Sec. 2. The zero of energy corresponds to the Fermi level. These parts of both bands which have considerable spectral weight  $n_{h,i}^{(1;2)}(k)$  are plotted by solid lines, those parts with small  $n_{h,i}^{(1;2)}(k) < 0.05$  by dotted lines.

Let us first discuss the dielectric (insulator) or heavily underdoped regimes which are represented by Figs. 1.1, 1.2 and 2.1, 2.2. In Figs. 1.1a and 1.2a the minimum of  $\epsilon_1(k)$  is close to the N-point and the spectrum is rather isotropic near the band bottom. The dispersions along the directions  $\Gamma-M$ , and  $\Gamma-X-M$  reproduce the ARPES results (compare for example Fig. 2.1 with the dispersion in Fig. 3 of Ref. [2]). The bandwidth of the first band  $W_1 = (4.4 - 3.3) = 0.44$  eV reflects also the experimental ARPES results  $W_1 = 0.2$  eV for  $\text{BiSr}_2\text{CaCuO}_{6+0.5}$  [2],  $W_1 = 0.3$  eV for  $\text{CaCuO}_2\text{Cl}_2$  [3], or  $W_1 = 0.35$  eV for  $\text{La}_2\text{CuO}_4$  [1]. Some of the uncertainty in these experimental values might be related to the drop of spectral weight near the  $\Gamma$ -point.

The most important result in the heavily underdoped regime is the sudden drop of spectral weight in the lowest band as  $k$  moves from N to M, see Figs. 1.1b and 1.2b. The position of the  $k$ -line where this drop occurs is close to that one which gives the remnant FS in the ARPES experiment [3]. The spin-polaron spectrum in Figs. 1.1a and 1.2a (2.1, 2.2) has a symmetry close to the symmetry of the magnetic BZ, but the spectral weight  $n_{h,i}^{(1)}(k)$  has the symmetry of the initial BZ, see Figs. 1.1b and 1.2b.

For the case  $p = 0.25$ ;  $x = 0.19$ , Figs. 1.6., 2.6, which we treat as close to optimal doping, a large FS centered at  $(\pi; \pi)$  is seen. It has a form consistent to the Luttinger theorem but with full filling  $(1+x)$ , not  $x$ . The spectral weight map from Fig. 1.6b demonstrates that such a large FS takes place due to small bare hole spectral weight at the spin-polaron  $k$ -states under the FS. The average value of  $n_{h,i}^{(1)}(k)$  is close to  $0.17 \pm 1$ . Let us note that the average value of  $n_{h,i}^{(1)}(k)$  for  $k$  below the FS would be approximately two times greater if we should take the local polaron approach, i.e. restrict the basis operator set to (11). One would lose even a qualitative correspondence to the experimental FS.

Let us compare the two lowest bands in the dielectric and the optimally doped cases along the N to  $\Gamma$  cut. In the former case, see Fig. 2.1, only the lowest hole polaron band is important (e.g. the upper electron one in Fig. 2.1), as the upper hole band has a small spectral weight. For the optimally doped case, Fig. 2.6, the second band is important as well. The correspondence to the ARPES experiment (see Fig. 3 in [2]) is good if we assume that parts of the spectra are missed where the spectral weight is small (dashed lines in Fig. 2.6) and if we treat the second band in the region close to  $\Gamma$  as an extension of the first one. Such a treatment is correct if we take into account the broadening of the bands. In our approach such a broadening would be equivalent to an additional splitting of bands due to additional operators (relative to the set (17), (18)). Such an improvement was investigated for the unfrustrated regular Kondo lattice model [37]. In the optimally doped case ( $p = 0.25$ ) the effective bandwidth  $W$  is  $W = \epsilon_{2\pi\text{max}} - \epsilon_F = 0.55$  eV, see Fig. 2.6, ( $W = 0.38$  eV for nearly optimally doped  $\text{BiSr}_2\text{CaCuO}_{6+}$  [2,48,49]).

The comparison with the dielectric state demonstrates some band narrowing with doping reduction as it is also given by ARPES [2].

An important feature of the spectrum is the presence of a second band  $\epsilon_2(k)$  well along the N to M cut, see Fig. 2.6. This branch resembles the main branch along the N to cut if we shift it in the  $k$ -space by  $Q$ . Relative to the main branch along the N to M cut the band  $\epsilon_2(k)$  is also shifted in energy by  $0.1 - 0.2$  eV. This branch is present as well in the underdoped case, see Fig. 2.4. An analogous branch (but without energy shift) was recently reported for underdoped Bi2212 [11] and it was treated as the shadow band first observed in Ref. [10]. For the optimally doped compounds the presence of this band can be important for the plasma frequency at about  $\omega_p = 1$  eV if one takes into account the corresponding interband transitions. Let us mention that in the ordinary band theory such transitions start at high energy  $> 1.2$  eV and lead only to a constant contribution in the static dielectric constant [50].

Our calculations reproduce also the extended saddle point which is stretched in the direction from X to close to the FS (see Fig. 1.6a). Such an extended saddle point is observed in the photoemission data of optimally doped compounds and there has been a lot of speculations that it is important to the physics of the superconductors [7]. Note that for this flat band region (close to  $(2=3;0)$ -point) the bare carrier spectral weight  $n_{h;}^{(1)}(k)$  is not small and is close to 0.22; see Fig. 1.6b.

The underdoped case is represented in Figs. 1.3, 2.3 with  $p = 0.15$ ,  $x = 0.06$  and in Figs. 1.4, 2.4 ( $p = 0.15$ ,  $x = 0.11$ ). As we move from doping 0.02 to doping 0.11 (compare in consecutive order Figs. 1.2b, 1.3b and 1.4b), the topology of lines with equal spectral weight changes dramatically. The remnant FS disappears, there appears finite spectral weight  $n_{h;}^{(1)}(k)$  close to the M point, the curvatures of lines change sign in a broad region and the spectral weight along the cut X  $(; =2)$  decreases. Between X and  $(; =2)$  the spectral weight is transferred to the second band. Since that is also the region where the FS crosses the X-M line with increasing doping, the  $n_{h;}^{(1)}(k)$  spectral weight along the FS is strongly changed. Such a strong decrease of spectral weight as  $k$  moves along the FS from the central region around N  $= ( =2; =2)$  to points close to X  $= (; 0)$  can be treated as the opening of a high energy pseudogap near the point  $(; 0)$ .

This pseudogap is often determined as  $\Delta = \epsilon_2(; 0) - \epsilon_f$  (see [3]). In our underdoped case ( $p = 0.15$ ;  $x = 0.11$ )  $n_{h;}^{(1)}(; 0)$  is small and the first band should be only weakly present at the X point in ARPES. So, we must treat  $\epsilon_2(; 0)$  as  $\epsilon_f(; 0)$  in the expression for the gap (see Table 1). Then for the adopted above value  $\Delta = 0.4$  eV the value of the pseudogap is equal to 0.19 eV in accordance with ARPES results (0.1 - 0.2 eV [2,12{14}]). The dependence of the spectral weight  $n_{h;}^{(1)}(; 0)$  on doping given in Table 1 is non monotonic. At first, a strong drop of  $n_{h;}^{(1)}(; 0)$  takes place in the underdoped region, but the spectral weight is sufficiently large in the optimally doped regime. Such a behavior reflects the ARPES scenario for a decreasing pseudogap as the doping increases from 0.1 to 0.2.

The evolution of the lowest band dispersion shows that in the just mentioned transition region also the formation of the extended saddle point takes place close to the  $(2=3;0)$ -point. As the doping increases above  $x = 0.11$  this flat band region is preserved.

For any doping, the particle spectral weight  $n_{h;}(k)^{(1)}$  for  $k$  close to the N point is large and nearly constant  $n_{h;}(k)^{(1)} = 0.22 - 0.25$ , see Table 1. And indeed, in this  $k$ -region the ARPES experiments demonstrate the position of the FS surface with a well pronounced quasiparticle peak. Accordingly, the second band in this  $k$ -region gives a small value  $n_{h;}(k)^{(2)} < 0.03$  (a small incoherent part) at any doping.

Table 1: Frustration parameter  $p$ , doping  $x$ , spin correlation length  $\xi_Q$  and cut-off momentum  $k_0$  for which calculations have been done. The derived energies  $\epsilon^{(1)}(k;0)$ ,  $\epsilon^{(2)}(k;0)$ , and  $\epsilon_F$  are given in units of  $t$ .  $n_{h;}(k)^{(1;2)}$  denotes the spectral weight of the first or second band, respectively.

$p$	$k_0$	$\xi_Q$	$x$	$n_{h;}(k;0)^{(1)}$	$n_{h;}(k;0)^{(2)}$	$n_{h;}(k=\pi/2; \pi/2)^{(1)}$	$\epsilon^{(1)}(k;0)$	$\epsilon^{(2)}(k;0)$	$\epsilon_F$
0.05	0.08	12	0.00	0.23	0.02	0.23	4.06		(-4.42)
0.10	0.17	6	0.02	0.25	0.00	0.26	4.09		4.38
0.13	0.30	3.4	0.06	0.13	0.11	0.27	4.21	4.04	4.34
0.15	0.35	< 3	0.11	0.06	0.18	0.23	4.38	4.03	4.40
0.2	0.35	< 2	0.14	0.08	0.16	0.24	4.35	4.08	4.40
0.25	0.35	< 1	0.19	0.10	0.13	0.25	4.28	4.10	4.36

## V. CONCLUSION

We presented a semi-phenomenological approach to describe the evolution of Fermi surface and electronic structure with doping. The approach is based on the spin-fermion model for the  $\text{CuO}_2$  plane and simulates the doping by a frustration term in the spin Hamiltonian. It shows a strong alteration of the electronic structure which is due to a simple and natural mechanism: doping leads to frustration in the spin subsystem and to the variation of spin-spin correlation functions, and correspondingly to the non-rigid behavior of the spectrum.

Our theory explains the isotropic band bottom, the large energy difference between N and X [1,2] and the remnant FS [3] of the undoped compounds. In the optimally doped case it shows a flat band region (an extended saddle point) between  $(\pi/2;0)$  and  $(0;0)$ , a large FS [5{9] and it shows signatures of a shadow FS [10,11]. We find in the underdoped region a rather strong change of dispersion and spectral weight at the FS near X. This finding can also be interpreted in terms of a pseudogap [12{14].

Our theoretical results would suggest for very low doping a FS in the form of small hole pockets (see e.g. Fig. 1.3 a). However, the spectral weights at those parts of the FS which are close to M are rather small. This might be a reason which hinders its

observation in ARPES. In underdoped samples we find a transition to a large FS but with very small spectral weight near  $X = (\pi; 0)$ . Accordingly, we would interpret the Fermi surface arcs [15] as those parts of the FS with large spectral weight. We find the parts of the FS with large spectral weight near to N to be remarkably stable with doping despite the tremendous changes in other parts of the BZ.

There are several possible improvements of the approach presented here. A straightforward way consists in introducing of several non overlapping domains  $\omega_1; \omega_2; \omega_3; \dots; \omega_i$  instead of the single domain  $\omega$  (see also [37]). As a result such an extension of the operator set should lead to a better description of the incoherent part of the spectral function. It might also lead to a better description of the shadow FS and to a more abrupt change of the spectral density along the FS in the underdoped case, i.e. a better description of the pseudogap.

#### ACKNOWLEDGMENTS

This work was supported, in part, by the INTAS (project No. 97-11066) and by RFFFS (projects No. 98-02-17187).

## Appendix A

Let us present the explicit form of Green's function  $G_s(k; \omega)$  and spin-wave spectrum  $\omega(k)$  for three degenerate modes in the framework of the spherically symmetric approach [45]:

$$G_s(k; \omega) = \langle S_k | \mathcal{S}_k \rangle = \frac{F(k)}{\omega^2 - \omega(k)^2}; \quad \omega = x; y; z \quad (27)$$

$$F(k) = \frac{1}{2} [J_1 z_g C_g (1 - \omega_g(k)) + J_2 z_d C_d (1 - \omega_d(k))] \quad (28)$$

$$\begin{aligned} \omega^2(k) = & \frac{2}{3} [(1 - \omega_g) J_1 J_2 K_{gd} + J_1^2 (z_g (z_g - 1) C_{g-1} + \frac{3}{4} z_g + K_{gg}) \\ & + (1 - \omega_d) J_1 J_2 K_{gd} + J_2^2 (z_d (z_d - 1) C_{d-3} + \frac{3}{4} z_d + K_{dd}) \\ & - \frac{1}{2} J_1^2 z_g^2 C_{g-1} - \frac{1}{2} J_2^2 z_d^2 C_{d-3} \\ & - (1 - \omega_g) J_1 J_2 z_g z_d C_{g-1} - (1 - \omega_d) J_1 J_2 z_g z_d C_{d-3}] \end{aligned} \quad (29)$$

$$K_{gd} = \sum_{r=g+d}^X r C_r; \quad K_{gg} = \sum_{r=g_1+g_2}^{g_1 \otimes g_2} r C_r; \quad K_{dd} = \sum_{r=d_1+d_2}^{d_1 \otimes d_2} r C_r;$$

Here  $z_g; z_d$  are a number of first and second nearest neighbors on square lattice and  $r$  are vertex corrections.

$$\begin{aligned}
g &= 1; \quad d = 3; \quad r = 2 \text{ if } r > d; \\
\frac{1}{2} \frac{1}{1} &= R = 0.863; \\
3 &= (1 - p) 2 + p 1; \\
J_1 &= (1 - p) J; J_2 = p J; \\
K_{gd} &= 8 C_g + 8 C_d; K_{gg} = 4 C_{2g} + 8 C_d; \\
K_{dd} &= 8 C_{2g} + 4 C_{2d};
\end{aligned}$$

The values of  $C_g, C_d, C_{2g}, C_{gd}, C_{2d}$  are calculated self-consistently for each values of  $p$  and  $T$  [45]. The equations (27,28,29) give an expression for the spin-spin structure factor  $C(k)$ :

$$C(k) = A (1 + e^{i k \cdot T}) = (e^{i k \cdot T} - 1); \quad A = F(k) = 2!_k: \quad (30)$$

The correlation length  $\xi_Q$  (relative to the Neel type phase) is determined by power expansion of the Green's function (27) on the value  $q = Q - k$  at  $\beta = 0$  [46]:

$$G(q;0) = G(Q;0) = (1 + \frac{2}{Q} q^2) \quad (31)$$

## Appendix B

Here we present the explicit form of  $K$  and  $D$  matrix elements. The following notations are used below.

$$D_{ij}(k) = \text{tr} [A_{k,ij} (\hat{\alpha} + \hat{J} + \hat{h})]; A_{k,ij}^+ g_i = \tilde{\alpha}_{ij} + J_1 J_{ij}^{(1)} + J_2 J_{ij}^{(2)} \tilde{h}_{ij};$$

$K_{ij}, \tilde{\alpha}_{ij}, J_{ij}^{(1)}, J_{ij}^{(2)}, \tilde{h}_{ij}$  are symmetric matrices.

$$g = 0.5(\cos k_x + \cos k_y); \quad d = \cos k_x \cos k_y; \quad 2g = 0.5(\cos 2k_x + \cos 2k_y);$$

The nonzero matrix elements are as follows:

$K$  matrix

$$\begin{aligned}
K_{11} &= 0.5(1 + \cos k_x); \\
K_{16} &= 0.5u(1 + \cos k_x); \\
K_{22} &= 0.5(1 + \cos k_y); \\
K_{26} &= 0.5u(1 + \cos k_y); \\
K_{33} &= 3 + 4 + C_g g; \\
K_{34} &= 0.5(u + u_g \cos k_x); \\
K_{35} &= 0.5(u + u_g \cos k_y); \\
K_{36} &= u + g C_g (v_g - v); \\
K_{44} &= 0.5(u + u_g \cos k_x); \\
K_{46} &= uv + 0.5w + 0.5 \cos k_x (v_g u - v u_g + w_g); \\
K_{55} &= 0.5(u + u_g \cos k_y); \\
K_{56} &= uv + 0.5w + 0.5 \cos k_y (v_g u - v u_g + w_g); \\
K_{66} &= (3+4)u + 2uv - w + g(u_g C_g + u^2 - (1=3)u_g^2 - 4C_g((1=3)u_g v + uv_g) \\
&\quad + 2vv_g C_g + 2v_g^2 C_g^2 + C_g v^2 (1 + (2=3)C_g)) - (2=3)g W_g^{(1)};
\end{aligned}$$



e m a t r i x

$$\begin{aligned}
11 &= 0.5(1 + \cos k_x)^2; \\
12 &= 0.5 + u_g + 0.5 u_d; \\
13 &= (3=2 + 2C_g u_g)(1 + \cos k_x); \\
14 &= (1 + \cos k_x)(u + u_g \cos k_x); \\
15 &= u(1 + \cos k_x) + u_g(\cos k_y + u_d); \\
16 &= (1 + \cos k_x)(u(1 + u_g) + 2C_g u_g(v_g - v)); \\
22 &= 0.5(1 + \cos k_y)^2; \\
23 &= (1 + \cos k_y)(3=2 + 2C_g u_g); \\
24 &= u(1 + \cos k_y) + u_g(\cos k_x + u_d); \\
25 &= (1 + \cos k_y)(u + u_g \cos k_y); \\
26 &= (1 + \cos k_y)(u(1 + u_g) + 2C_g u_g(v_g - v)); \\
33 &= 9=8 - 4C_g u_g + C_g + 0.5C_{2g} u_{2g} + C_d u_d; \\
34 &= (3=4)u - 0.5v_g u_y \cos k_x + (\cos^2 k_x - 0.5)(v_g C_g + 0.5u_{2g}) \\
&\quad + u_g(u_g + 2v_g C_g - 2v_g C_g \cos k_x - 2v_g C_g) + u_d(0.5u_d + v_d C_g); \\
35 &= (3=4)u - 0.5v_g u_y \cos k_y + (\cos^2 k_y - 0.5)(v_g C_g + 0.5u_{2g}) \\
&\quad + u_g(u_g + 2v_g C_g - 2v_g C_g \cos k_y - 2v_g C_g) + u_d(0.5u_d + v_d C_g); \\
36 &= (9=2)u - (1=4)u_y + u_g(3u + 4v_g C_g + 3u_g - 4v_g C_g) \\
&\quad + u_{2g}(C_g u + 0.5v_{2g} C_{2g} - (2=3)v_g C_g C_{2g} - 0.5v_{2g} C_{2g} \\
&\quad - (2=3)v_g C_{2g} - (1=3)u_y C_{2g} - 2v_g C_g^2 + u_{2g} C_g) \\
&\quad + u_d(2C_g u + v_d C_d - v_d C_d - (4=3)C_g C_d(v_d + v) - (2=3)u_y C_d - 4v_g C_g^2 + 2u_d C_g); \\
44 &= (3=4)u - v_g u_g - 2uv + w + 0.5w_g^{(1)} + \cos k_x(u_g - 2v_g u_y - 2v_g u + 2w_g) \\
&\quad + (\cos^2 k_x - 0.5)((1=2)u_{2g} - 2v_g u_g + w_g^{(2)}); \\
45 &= 0.5u + 2u_g(v_g u_y - v_g u + w_g + 0.5u_g) - 2uv + w + u_d(0.5u_d - 2u_y v_g + w_g^{(3)}); \\
46 &= 1.5uv + 1.5u - 0.75w + 0.5(u C_g + C_g v^2 + C_g v v_g + C_g v_g^2 - (8=3)u_y v_g C_g \\
&\quad + (2=3)u u_g - (8=3)u v C_g + (8=3)v v_g C_g^2 - (1=3)W_1^{(1)}) \\
&\quad + u_g(v_g u - v_g u_y + w_g + 2u_g C_g + 2v_g^2 C_g + (4=3)v^2 C_g^2 + 4v v_g C_g + 4v_g^2 C_g^2 \\
&\quad + 2u^2 - (2=3)u_y^2 - (8=3)u_y v C_g - 8u_y v_g C_g - (4=3)W_3^{(1)}) \\
&\quad + \cos k_x(w_g + 1.5u_g + uv_g + u_g v) \\
&\quad + (2\cos^2 k_x - 1)(0.25w_{2g} - 0.25u v_{2g} - 0.25v u_{2g} + 0.5C_g u_{2g} + 0.5C_g v v_{2g} \\
&\quad + C_g^2 v_g v_{2g} - (1=3)C_g u_{2g} v - C_g u v_{2g} - (1=6)u_y u_{2g} + 0.5C_g v v_g + 0.5C_g v_g^2 \\
&\quad + (1=3)C_g^2 v v_g - (4=3)C_g u_g v_g + 0.5u u_g - (1=3)W_2^{(1)}) \\
&\quad + 2u_d(0.25w_d - 0.25u v_d - 0.25v u_d + 0.5C_g u_d + 0.5C_g v v_d + C_g^2 v_g v_d - (1=3)C_g u_d v \\
&\quad - C_g u v_d - (1=6)u_y u_d + 0.5C_g v v_g + 0.5C_g v_g^2 + (1=3)C_g^2 v v_g - (4=3)C_g u_g v_g \\
&\quad + 0.5u u_g - (1=3)W_3^{(1)}); \\
55 &= (3=4)u - v_g u_g - 2uv + w + 0.5w_g^{(1)} + \cos k_y(u_g - 2v_g u_y - 2v_g u + 2w_g) \\
&\quad + (\cos^2 k_y - 0.5)((1=2)u_{2g} - 2v_g u_g + w_g^{(2)}); \\
56 &= 1.5uv + 1.5u - 0.75w + 0.5(u C_g + C_g v^2 + C_g v v_g + C_g v_g^2 - (8=3)u_y v_g C_g
\end{aligned}$$

$$\begin{aligned}
& + (2=3)uu_g \quad (8=3)uvC_g + (8=3)vv_gC_g^2 \quad (1=3)W_1^{(')} \\
& + {}_g(v_u \quad v_u + w_g + 2u_gC_g + 2v^2C_g + (4=3)v^2C_g^2 + 4vv_gC_g + 4v_g^2C_g^2 \\
& + 2u^2 \quad (2=3)u_g^2 \quad (8=3)u_gvC_g \quad 8u_gv_gC_g \quad (4=3)W_g^{(')} \\
& + \cos k_y (w_g + 1.5u_g + uv_g + u_gv) \\
& + (2 \cos^2 k_y - 1) (0.25w_{2g} \quad 0.25u_{2g} \quad 0.25v_{2g} + 0.5C_gu_{2g} + 0.5C_gvv_{2g} \\
& + C_g^2v_gv_{2g} \quad (1=3)C_gu_{2g}v \quad C_guv_{2g} \quad (1=6)u_gu_{2g} + 0.5C_gvv_g + 0.5C_gv_g^2 \\
& + (1=3)C_g^2vv_g \quad (4=3)C_gu_gv_g + 0.5uu_g \quad (1=3)W_2^{(')} \\
& + 2_d(0.25w_d \quad 0.25u_d \quad 0.25v_d + 0.5C_gu_d + 0.5C_gvv_d + C_g^2v_gv_d \quad (1=3)C_gu_dv \\
& \quad C_guv_d \quad (1=6)u_gu_d + 0.5C_gvv_g + 0.5C_gv_g^2 + (1=3)C_g^2vv_g \quad (4=3)C_gu_gv_g \\
& + 0.5uu_g \quad (1=3)W_3^{(')}); \\
66 = & \quad 9vu \quad (9=8)u + (9=2)w \quad (1=4)W_g^{(1)} + u(C_g + (2=3)u_g \quad (8=3)C_gv) \\
& + v^2C_g + v_g^2C_g + vv_g(C_g + (8=3)C_g^2) + v_g(0.5u_g \quad (8=3)C_gu_g) \quad (2=3)W_1^{(')} \\
& + {}_g(vu_g(6 + (16=3)C_g) + v_gu(6 + 16C_g) \quad 8vv_gC_g \quad v^2(4C_g + (8=3)C_g^2) \quad 4u^2 \\
& + (4=3)u_g^2 \quad 8v_g^2C_g^2 \quad 4u_gC_g + 6w_g + (8=3)W_g^{(')} \\
& + {}_{2g}(0.5u_{2g}C_{2g} + vv_{2g}(C_{2g} + (4=3)C_gC_{2g}) + v^2(0.5C_{2g} + (4=3)C_gC_{2g} + (1=3)C_{2g}^2) \\
& + v_{2g}^2(C_{2g}^2 + (8=3)C_gC_{2g}) + v((2=3)u_gC_{2g} + (2=3)u_gC_{2g} \quad 2u_gC_g \quad 2u_gC_g) \\
& \quad v_{2g}(2u_{2g}C_g + (2=3)u_gC_{2g} + (2=3)u_{2g}C_g + 2u_gC_g) + 0.5u^2 \quad (1=6)M_{2g}^2 \quad (14=3)v_g^2C_g^2 \\
& + vv_g(4C_g^2 \quad (4=3)C_gC_{2g}) + v_gv_{2g}(8=3)(C_g^2 \quad C_gC_{2g}) + v_g((2=3)u_gC_{2g} + (2=3)u_{2g}C_g \\
& + 2u_gC_g) + 2w_{2g}C_g \quad (1=3)w_g^{(2)}C_{2g} \quad (1=3)W_{2g}^{(')} \\
& + 2_d(0.5u_dC_d + vv_d(C_d + (4=3)C_gC_d) + v^2(0.5C_d + (4=3)C_gC_d + (1=3)C_d^2) \\
& + v_d^2(C_d^2 + (8=3)C_gC_d) + v((2=3)u_dC_d + (2=3)u_gC_d \quad 2u_dC_g \quad 2u_gC_g) \\
& \quad v_d(2u_dC_d + (2=3)u_gC_d + (2=3)u_dC_g + 2u_gC_g) + 0.5u^2 \quad (1=6)u_d^2 \quad (14=3)v_g^2C_g^2 \\
& + vv_g(4C_g^2 \quad (4=3)C_gC_d) + v_gv_d(8=3)(C_g^2 \quad C_gC_d) + v_g((2=3)u_gC_d + (2=3)u_dC_g \\
& + 2u_gC_g) + 2w_dC_g \quad (1=3)w_g^{(3)}C_d \quad (1=3)W_d^{(')});
\end{aligned}$$

$\mathfrak{F}^{(1)}$  matrix

$$\begin{aligned}
J_{33} &= 4C_g + C_g \quad {}_g; \\
J_{34} &= 2C_g(v_g \quad v) + \cos k_x C_g(0.5v \quad 2v_g + 0.5v_{2g} + v_d); \\
J_{35} &= 2C_g(v_g \quad v) + \cos k_y C_g(0.5v \quad 2v_g + 0.5v_{2g} + v_d); \\
J_{36} &= 2C_g(v \quad v_g) + 2u_g + {}_g(0.5C_g(v_g \quad v) \quad 2C_g^2v_g \quad 0.5u_g \quad (2=3)u_gC_{2g} \\
& \quad (4=3)u_gC_d + (4=3)v_dC_gC_d + (2=3)v_{2g}C_gC_{2g} + (2=3)u_{2g}C_g + (4=3)u_dC_g); \\
J_{44} &= 2C_g(v_g \quad v) + C_g \cos k_x(0.5v \quad 2v_g + 0.5v_{2g} + v_d); \\
J_{46} &= (4=3)C_g(w_g \quad w) + (4=3)C_gu(v \quad v_g) + v_g^2(C_g + (4=3)C_g^2) + 2v^2C_g + (4=3)W_{g^4}^{(J)} \\
& + vv_gC_g(3 \quad (4=3)C_g) + 0.5 \cos k_x((8=3)u_g^2 \quad (2=3)u^2 \quad (2=3)u_{2g} \quad (4=3)u_{2g} \\
& + (8=3)uv_gC_g \quad (8=3)u_gv_gC_g + (2=3)uv_gC_g + (2=3)u_{2g}v_gC_g + (4=3)u_dv_gC_g \\
& \quad (2=3)u_gvC_g \quad (2=3)u_gv_{2g}C_g \quad (4=3)u_gv_dC_g + 4v_g^2C_g(0.5 \quad (2=3)C_g) \\
& + 4vv_gC_g \quad v^2C_g \quad vv_gC_g \quad 2vv_dC_g + v_gv(0.5C_g + (2=3)C_g^2) \\
& + v_gv_{2g}C_g(0.5 + (2=3)C_g) + 2v_gv_dC_g(0.5 + (2=3)C_g) \\
& + (2=3)C_g(w_g^{(2)} + w_g^{(1)} + 2w_g^{(3)} \quad 4C_gw_g) + (4=3)W_{g^3}^{(J)}); \\
J_{55} &= 2C_g(v_g \quad v) + C_g \cos k_y(0.5v \quad 2v_g + 0.5v_{2g} + v_d); \\
J_{56} &= (4=3)C_g(w_g \quad w) + (4=3)C_gu(v \quad v_g) + v_g^2(C_g + (4=3)C_g^2) + 2v^2C_g + (4=3)W_{g^4}^{(J)} \\
& + vv_gC_g(3 \quad (4=3)C_g) + 0.5 \cos k_y((8=3)u_g^2 \quad (2=3)u^2 \quad (2=3)u_{2g} \quad (4=3)u_{2g}
\end{aligned}$$

$$\begin{aligned}
& + (8=3)uv_g C_g \quad (8=3)u_g v_g C_g + (2=3)uv_g C_g + (2=3)u_{2g} v_g C_g + (4=3)u_d v_g C_g \\
& \quad (2=3)u_g v C_g \quad (2=3)u_g v_{2g} C_g \quad (4=3)u_g v_d C_g + 4v_g^2 C_g (0.5 \quad (2=3)C_g) \\
& + 4vv_g C_g \quad v^2 C_g \quad vv_g C_g \quad 2vv_d C_g + v_g v (0.5 C_g + (2=3)C_g^2) \\
& + v_g v_{2g} C_g (0.5 + (2=3)C_g) + 2v_g v_d C_g (0.5 + (2=3)C_g) \\
& + (2=3)C_g (w_g^{(2)} + w_g^{(1)} + 2w_g^{(3)} \quad 4C_g w_g) + (4=3)W_{g3}^{(J)}); \\
F 0 = & \quad 4u C_g \quad (8=3)uu_g + 8C_g uv + (8=3)w C_g \quad (8=3)w_g C_g + v_g u_g ((32=3)C_g \quad 4) + 2w_g^{(1)} \\
& + (8=3)v_g u C_g + 3v_g C_g \quad 3v C_g \quad 8v^2 C_g \quad 6v_g^2 C_g \quad (8=3)v_g^2 C_g^2 + 2vv_g C_g \quad 8C_g^2 vv_g \\
& + (8=3)(W_1^{(1)} \quad W_{g1}^{(J)} \quad W_{g2}^{(J)}); \\
F 1 = & \quad (2=3)u^2 + u_g C_g \quad (10=3)uv_g C_g \quad 2u_g v C_g + 0.5u_g v + 0.5uv_g + v^2 C_g (0.75 + C_g) \\
& + v_g^2 C_g (0.25 + (5=3)C_g) + 2vv_g C_g \quad 0.5w_g \quad (2=3)w_g (C_{2g} + 2C_d) + uv C_g \quad uv_g C_g \\
& \quad (2=3)u_g v_g C_g + (2=3)u_g v C_{2g} \quad (2=3)u_g v C_g + (2=3)uv C_{2g} + u_g v_g C_g + (2=3)uv_g C_{2g} \\
& \quad u_g v_{2g} C_g \quad (2=3)uv_g C_{2g} + (2=3)v^2 C_g (C_g \quad C_{2g}) + v_g^2 C_g ((5=3)C_g \quad (7=3)C_{2g}) \\
& \quad (8=3)vv_g C_g^2 + vv_{2g} C_g ((5=3)C_{2g} + C_g) + 4v_g v_{2g} C_g C_{2g} + 2(uv C_g \quad uv_g C_g \\
& \quad (2=3)u_d v_g C_g + (2=3)u_g v C_d \quad (2=3)u_g v C_g + (2=3)uv C_d + u_g v_g C_g + (2=3)uv_g C_d \\
& \quad u_g v_d C_g \quad (2=3)uv_d C_d + (2=3)v^2 C_g (C_g \quad C_d) + v_g^2 C_g ((5=3)C_g \quad (7=3)C_d) \\
& \quad (8=3)vv_g C_g^2 + vv_d C_g ((5=3)C_d + C_g) + 4v_g v_d C_g C_d + 2=3C_g (w_{g2g}^{(1)} + 2w_{gd}^{(1)}) \\
& \quad (2=3)W_g^{(1)}); \\
F 2 = & \quad 3u_g v_g C_g + 3uv_g C_g + (2=3)uv_g C_{2g} + (2=3)u_{2g} v_g C_g \quad (2=3)uv_g C_{2g} \quad u_g v_{2g} C_g \\
& \quad 3uv C_g \quad (2=3)u_g v C_g + (4=3)u_d v_g C_g \quad (4=3)uv_d C_d \quad 2u_g v_d C_g \quad (4=3)u_d v C_g \\
& + (4=3)uv_g C_d + 0.5uv_g \quad 0.5uv + C_g^2 (v_{2g} + v + 2v_d \quad 4v_g) + v^2 ((11=3)C_g^2 \\
& \quad 0.25C_g + (2=3)C_{2g} C_g + (4=3)C_g C_d) + v_g^2 ((50=3)C_g^2 \\
& \quad (7=3)(C_g C_{2g} \quad (14=3)C_g C_d \quad 0.25C_g) + vv_g ((52=3)C_g^2 + 0.5C_g \\
& \quad (2=3)C_g C_{2g} \quad (4=3)C_g C_d) + v_g v_{2g} ((8=3)C_g^2 + (4=3)C_g C_{2g}) \\
& + vv_{2g} ((5=3)C_g^2 + C_g C_{2g}) + v_g v_d ((8=3)C_g C_d + (16=3)C_g^2) \\
& + vv_d ((10=3)C_g^2 + 2C_g C_d) + (1=6)W_g^{(J)}; \\
J_{66} = & F 0 + \quad_g (F 1 + F 2);
\end{aligned}$$

$\mathfrak{g}^{(2)}$  matrix

$$\begin{aligned}
Jd_{33} &= \quad 4C_d; \\
Jd_{34} &= 2C_d (v_d \quad v) + \cos k_x C_d (v_g + v_f \quad 2v_g); \\
Jd_{35} &= 2C_d (v_d \quad v) + \cos k_y C_d (v_g + v_f \quad 2v_g); \\
Jd_{36} &= 2C_d (v \quad v_d) + 2u_d + (4=3) \quad_g (C_d (C_g v_g + C_f v_f) \quad 2C_g C_d v_g + C_g (u_g + u_f) \\
& \quad u_g (C_g + C_f)); \\
Jd_{44} &= 2C_d (v_d \quad v) + \cos k_x (C_d (v_g + v_f) \quad 2C_d v_g); \\
Jd_{55} &= 2C_d (v_d \quad v) + \cos k_y (C_d (v_g + v_f) \quad 2C_d v_g); \\
Jd_{64} &= (4=3)uC_d (v \quad v_d) + (4=3)C_d (w_d \quad w) + 2v^2 C_d + v_d^2 (C_d + (4=3)C_d^2) + (4=3)W_{d4}^{(J)} \\
& \quad vv_d (3C_d + (4=3)C_d^2) + \cos k_x ((4=3)C_d (uv_g \quad u_g v_d) + (4=3)u_g u_d \quad (4=3)C_d w_{2g} \\
& + v_g v_d (C_d \quad (4=3)C_d^2) + 2C_d v_g (v \quad v_d) \quad (2=3)u (u_g + u_f) + (2=3)C_d (v_d (u_g + u_f) \\
& \quad u_d (v_g + v_f)) + ((2=3)C_d^2 + 0.5C_d) v_d (v_g + v_f) \quad C_d v (v_g + v_f) \\
& + (2=3)C_d (w_{gd}^{(2)} + w_{gd}^{(1)}) + (4=3)W_{d3}^{(J)}); \\
Jd_{65} &= (4=3)uC_d (v \quad v_d) + (4=3)C_d (w_d \quad w) + 2v^2 C_d + v_d^2 (C_d + (4=3)C_d^2) + (4=3)W_{d4}^{(J)} \\
& \quad vv_d (3C_d + (4=3)C_d^2) + \cos k_y ((4=3)C_d (uv_g \quad u_g v_d) + (4=3)u_g u_d \quad (4=3)C_d w_g
\end{aligned}$$

$$\begin{aligned}
& + v_g v_d (C_d - (4=3)C_d^2) + 2C_d v_g (v - v_d) - (2=3)u (u_g + u_f) + (2=3)C_d (v_d (u_g + u_f) \\
& \quad u_d (v_g + v_f)) + ((2=3)C_d^2 + 0.5C_d)v_d (v_g + v_f) - C_d v (v_g + v_f) \\
& + (2=3)C_d (w_{gd}^{(2)} + w_{gd}^{(1)}) + (4=3)W_{d3}^{(J)}); \\
F_{d0} = & 4u C_d - (8=3)u u_d + 8C_d u v + (8=3)w C_d - (8=3)w_d C_d + v_d u_d ((32=3)C_d - 4) \\
& + (8=3)v_d u C_d + 3v_d C_d - 3v C_d - 8v_d^2 C_d - 6v_d^2 C_d - (8=3)v_d^2 C_d^2 + 2v v_d C_d - 8C_d^2 v v_d \\
& + 2w_{dd}^{(1)} + (8=3)(W_1^{(1)} - W_{d1}^{(J)} - W_{d2}^{(J)}); \\
F_{d1} = & (4=3)w_g (C_g + C_f) + (4=3)C_g (w_{gd}^{(1)} + w_{fd}^{(1)}) + u v (4C_d + (4=3)(C_g + C_f)) \\
& + (4=3)u_g v (C_g + C_f) - (8=3)u_d v C_g - 4u v_d C_d + (4=3)u v_g (C_g + C_f) \\
& (4=3)u (v_g C_g + v_f C_f) - (4=3)v_d C_g (u_g + u_f) + (4=3)u_g v_g C_d + (8=3)u_d v_g C_g \\
& (4=3)u_d C_g (v_g + v_f) - (2=3)u_g C_d (v_g + v_f) + v^2 ((8=3)C_g C_d - (4=3)C_g (C_g + C_f)) \\
& (32=3)v v_g C_g C_d + 2v C_g C_d (v_g + v_f) - (10=3)v C_d (v_g C_g + v_f C_f) + v_g v_d ((20=3)C_g C_d \\
& 2C_d (C_g + C_f)) + (8=3)C_g v_g (v_g C_g + v_f C_f) + (16=3)v_d C_d (v_g C_g + v_f C_f) \\
& (8=3)v_d^2 C_g (C_g + C_f) + v v_d ((4=3)C_g (C_g + C_f) - (4=3)C_d (C_g + C_f)); \\
F_{d2} = & v^2 ((8=3)C_g C_d + (4=3)C_g (C_g + C_f)) + 16C_g C_d v v_g - 4C_d u v + 2v v_g C_g C_d \\
& + 2v v_f C_d C_f - (10=3)v C_d C_g (v_g + v_f) - (4=3)C_g (u_g + u_f) v + (4=3)C_d u_g v_g \\
& + (8=3)C_g u_d v_g + (4=3)(C_g + C_f) u v_g - v_g v_d (20C_g C_d + 2C_d (C_g + C_f)) \\
& (8=3)C_g (C_g + C_f) v_g^2 + v v_d ((8=3)C_g C_d - (4=3)C_g (C_g + C_f)) + 4C_d u v_d \\
& + v_d C_d (2C_g (v_g + v_f) - 2(v_g C_g + v_f C_f)) + (4=3)C_g (u_g + u_f) v_d - (2=3)C_d u_g (v_g + v_f) \\
& (4=3)u (C_g v_g + C_f v_f) - (4=3)C_g u_d (v_g + v_f) + (10=3)C_g C_d v_d (v_g + v_f) + (1=6)W_d^{(J)} \\
& + 2C_d v_d (C_g v_g + C_f v_f) + (8=3)C_g v_g (C_g v_g + C_f v_f) - 4C_g C_d v_g + 2C_g C_d (v_g + v_f); \\
J_{d66} = & F_{d0} + \frac{1}{g} (F_{d1} + F_{d2});
\end{aligned}$$

Final matrix

$$\begin{aligned}
h_{12} &= 2(0.5 + \frac{1}{g} + 0.5 \frac{1}{d}); \\
h_{16} &= 2u(0.5 + \frac{1}{g} + 0.5 \frac{1}{d}); \\
h_{26} &= h_{16}; \\
h_{33} &= 2(3=4 + 2C_g \frac{1}{g} + C_d \frac{1}{d}); \\
h_{34} &= 2(0.5u + u_g \frac{1}{g} + 0.5u_d \frac{1}{d}); \\
h_{35} &= h_{34}; \\
h_{36} &= 2(u + 2C_g \frac{1}{g} (v_g - v) + C_d \frac{1}{d} (v_d - v)); \\
h_{45} &= h_{34}; \\
h_{46} &= 2(uv + \frac{1}{g} (w_g - u_g v - v_g u) + 0.5w + 0.5 \frac{1}{d} (w_d - u v_d - u_d v)); \\
h_{56} &= h_{46}; \\
h_{66} &= 2((3=4)u + 2uv - w + \frac{1}{g} (2C_g u_g + 2C_g (v^2 + 2v_g v) + (4=3)C_g^2 (v^2 + 3v_g^2) \\
& + 2u^2 - (2=3)u_g^2 - 8C_g ((1=3)u_g v + u v_g)) - (4=3)\frac{1}{g} W_g^{(1)} + \frac{1}{d} (C_d u_d + C_d (v^2 + 2v v_d) \\
& + (2=3)C_d^2 (v^2 + 3v_d^2) - 4C_d ((1=3)u_d v + u v_d) + u^2 - (1=3)u_d^2) - (2=3)\frac{1}{d} W_d^{(1)});
\end{aligned}$$

Above the following notations are taken

$$\begin{aligned}
v &= \frac{1}{N} \frac{P}{1}; \quad \frac{1}{N} \frac{P}{2} \\
v_1 &= \frac{1}{N} \frac{P}{e^{i1}}; \quad 1 = g; d; 2g; f; \\
u &= \frac{1}{N} \frac{P}{C};
\end{aligned}$$

$$\begin{aligned}
u_1 &= \frac{1}{N} \sum_{\mathbf{l}} e^{i\mathbf{l} \cdot \mathbf{r}_1} C_{\mathbf{l}}; \quad \mathbf{l} = \mathbf{g}; \mathbf{d}; 2\mathbf{g}; \mathbf{f}; \\
w &= \frac{1}{N^2} \sum_{\mathbf{l}_1, \mathbf{l}_2} e^{i\mathbf{l}_1 \cdot \mathbf{r}_1 + i\mathbf{l}_2 \cdot \mathbf{r}_2} C_{\mathbf{l}_1} C_{\mathbf{l}_2}; \\
w_1 &= \frac{1}{N^2} \sum_{\mathbf{l}_1, \mathbf{l}_2} e^{i\mathbf{l}_1 \cdot \mathbf{r}_1 + i\mathbf{l}_2 \cdot \mathbf{r}_2} C_{\mathbf{l}_1} C_{\mathbf{l}_2}; \quad \mathbf{l}_1, \mathbf{l}_2 = \mathbf{g}; \mathbf{d}; 2\mathbf{g}; \\
w_{\mathbf{l}_1 \mathbf{l}_2}^{(m)} &= \frac{1}{N^2} \sum_{\mathbf{l}_1, \mathbf{l}_2} e^{i\mathbf{l}_1 \cdot \mathbf{r}_1 + i\mathbf{l}_2 \cdot \mathbf{r}_2} C_{\mathbf{l}_1} C_{\mathbf{l}_2}; \quad \mathbf{l}_1, \mathbf{l}_2 = \mathbf{g}; \mathbf{d}; 2\mathbf{g}; \mathbf{f}; \\
m &= 1: \mathbf{l}_1 \mathbf{l}_2 > 0; m = 2: \mathbf{l}_1 \mathbf{l}_2 < 0; m = 3: \mathbf{l}_1 \mathbf{l}_2 = 0; \\
w_1^{(m)} &= w_{\mathbf{l}_1 \mathbf{l}_2}^{(m)} (\mathbf{l}_1 = \mathbf{l}_2); \\
W_1^{( )} &= \frac{1}{N^2} \sum_{\mathbf{l}_1, \mathbf{l}_2} e^{i(\mathbf{l}_1 - \mathbf{l}_2) \cdot \mathbf{r}_1} e^{i\mathbf{l}_2 \cdot \mathbf{r}_2} C_{\mathbf{l}_1} C_{\mathbf{l}_2}; \quad \mathbf{l} = \mathbf{g}; \mathbf{d}; 2\mathbf{g}; \\
W_1^{( )} &= \frac{1}{N^2} \sum_{\mathbf{l}_1, \mathbf{l}_2} e^{i(\mathbf{l}_1 - \mathbf{l}_2) \cdot \mathbf{r}_1} C_{\mathbf{l}_1} C_{\mathbf{l}_2}; \\
W_2^{( )} &= \frac{1}{N^2} \sum_{\mathbf{l}_1, \mathbf{l}_2} e^{i(\mathbf{l}_1 + \mathbf{l}_2) \cdot \mathbf{r}_1} e^{i(\mathbf{l}_1 - \mathbf{l}_2) \cdot \mathbf{r}_2} C_{\mathbf{l}_1} C_{\mathbf{l}_2}; \\
W_3^{( )} &= \frac{1}{N^2} \sum_{\mathbf{l}_1, \mathbf{l}_2} e^{i\mathbf{l}_1 \cdot \mathbf{r}_1} e^{i\mathbf{l}_2 \cdot \mathbf{r}_2} C_{\mathbf{l}_1} C_{\mathbf{l}_2}; \\
W_{11}^{(J)} &= \frac{1}{N^2} \sum_{\mathbf{l}_1, \mathbf{l}_2} e^{i\mathbf{l}_1 \cdot \mathbf{r}_1} e^{i\mathbf{l}_2 \cdot \mathbf{r}_2} C_{\mathbf{l}_1} C_{\mathbf{l}_2}; \quad \mathbf{l} = \mathbf{g}; \mathbf{d}; \\
W_{12}^{(J)} &= \frac{1}{N^2} \sum_{\mathbf{l}_1, \mathbf{l}_2} e^{i(\mathbf{l}_1 - \mathbf{l}_2) \cdot \mathbf{r}_1} C_{\mathbf{l}_1} C_{\mathbf{l}_2}; \quad \mathbf{l} = \mathbf{g}; \mathbf{d}; \\
W_{13}^{(J)} &= \frac{1}{N^2} \sum_{\mathbf{l}_1, \mathbf{l}_2} e^{i\mathbf{l}_1 \cdot \mathbf{r}_1} e^{i\mathbf{l}_2 \cdot \mathbf{r}_2} (C_{\mathbf{l}_1} C_{\mathbf{l}_2} - C_{\mathbf{l}_1} C_{-\mathbf{l}_2}) C_{\mathbf{l}_1} C_{\mathbf{l}_2}; \quad \mathbf{l} = \mathbf{g}; \mathbf{d}; \\
W_{14}^{(J)} &= \frac{1}{N^2} \sum_{\mathbf{l}_1, \mathbf{l}_2} (C_{\mathbf{l}_1} C_{\mathbf{l}_2} - C_{\mathbf{l}_1} C_{-\mathbf{l}_2}) C_{\mathbf{l}_1} C_{\mathbf{l}_2}; \quad \mathbf{l} = \mathbf{g}; \mathbf{d}; \\
W_1^{(J)} &= \frac{1}{N^2} \sum_{\mathbf{l}_1, \mathbf{l}_2} e^{i\mathbf{l}_1 \cdot \mathbf{r}_1} e^{i\mathbf{l}_2 \cdot \mathbf{r}_2} (C_{\mathbf{l}_1} C_{\mathbf{l}_2} + C_{\mathbf{l}_1} C_{-\mathbf{l}_2}) \\
&\quad e^{i(\mathbf{l}_1 - \mathbf{l}_2) \cdot \mathbf{r}_1} e^{i\mathbf{l}_2 \cdot \mathbf{r}_2} C_{\mathbf{l}_1} C_{\mathbf{l}_2} + e^{i(\mathbf{l}_1 - \mathbf{l}_2) \cdot \mathbf{r}_1} e^{i\mathbf{l}_1 \cdot \mathbf{r}_2} C_{\mathbf{l}_1} C_{\mathbf{l}_2}); \quad \mathbf{l} = \mathbf{g}; \mathbf{d};
\end{aligned}$$


---

- [1] B.O.Wells, Z.X.Shen, A.Matsuura, et al, Phys.Rev.Lett. 74, 964 (1995).
- [2] D.S.Marshall, D.S.Dessau, A.G.Loesser, et al, Phys.Rev.Lett. 76, 4841 (1996).
- [3] F.Ronning, C.Kim, D.L.Feng, et al, Science 282, 2067 (1998).
- [4] A.P.Kampf and J.R.Schrieffer, Phys.Rev.B 42, 7967 (1990).
- [5] J.G.Tobin, C.G.Olson, C.Gu, et al, Phys.Rev.B 45, 5563 (1992).
- [6] K.Gofron, J.C.Campanozano, H.Ding, et al, J.Phys.Chem.Solids 54, 1193 (1993).
- [7] A.A.Abrikosov, J.C.Campanozano and J.C.Gofron, Physica C 214, 73 (1993).
- [8] D.S.Dessau, Z.X.Shen, D.M.King, et al, Phys.Rev.Lett. 71, 278 (1993).
- [9] D.M.King, Z.H.Shen, D.S.Dessau, et al, Phys.Rev.Lett. 73, 3298 (1994).

- [10] P. Aebi, J. Osterwalder, P. Schwaller, et al., *Phys. Rev. Lett.* 72, 2757 (1994).
- [11] V. Borisenko, M. S. Golden, S. Legner, et al., *Phys. Rev. Lett.* 84, 4453 (2000).
- [12] A. G. Loeser, Z. X. Shen, D. S. Dessau, et al., *Science* 273, 325 (1996).
- [13] H. Ding, T. Yokoya, J. C. Cam puzano, et al., *Nature*, 382, 51 (1996).
- [14] H. Ding, M. R. Norman, T. Yokoya, T. Takeuchi, et al., *Phys. Rev. Lett.* 78, 2628 (1997).
- [15] M. R. Norman, H. Ding, M. Randeria, et al., *Nature* 392, 157 (1998).
- [16] K. J. Szczepanski, P. Horsch, W. Stephan, M. Ziegler, *Phys. Rev. B* 41, 2017 (1990).
- [17] E. Dagotto, R. Joynt, A. Moreo, S. Bacci and Gagliano E., *Phys. Rev. B* 41, 9049 (1990).
- [18] D. Du y, A. Nazarenko, S. Haas, et al., *Phys. Rev. B* 56, 5599 (1997).
- [19] C. L. Kane, P. A. Lee and N. Read, *Phys. Rev. B* 39, 6880 (1989).
- [20] G. Martinez and P. Horsch, *Phys. Rev. B* 44, 317 (1991).
- [21] T. Toyama, Y. Sibata, S. Maekawa, et al., *J. Phys. Soc. Jpn.* 69, 9 (2000).
- [22] R. Eder and K. Becker, *Z. Phys. B* 78, 219 (1990).
- [23] C. E. Cameiro, M. J. De Oliveira, S. R. A. Salinas and G. V. Uimin, *Physica C* 166, 206 (1990).
- [24] A. V. Chubukov, and D. K. Morr, *Phys. Rep.* 288, 355 (1997).
- [25] R. Eder, Y. Ohta, and G. A. Sawatzky, *Phys. Rev. B* 55, R3414 (1997).
- [26] C. Kim, P. J. White, Z. X. Shen, et al., *Phys. Rev. Lett.* 80, 4245 (1998).
- [27] W. Yin, C. Gong and P. Leung, *Phys. Rev. Lett.* 81, 2534 (1998).
- [28] V. J. Emery, *Phys. Rev. Lett.* 58, 2794 (1987).
- [29] V. J. Emery and G. Reiter, *Phys. Rev. B* 38, 4547 (1988).
- [30] M. Inui, S. Doniach and M. Gabay, *Phys. Rev. B* 38, 6631 (1988).
- [31] J. F. Annet, R. M. Martin, A. K. Mc Mahan and S. Satpathy, *Phys. Rev. B* 40, 2620 (1989).
- [32] S. Bacci, E. Gagliano, and F. Nori, *Int. J. Mod. Phys. B* 5, 325 (1991).
- [33] A. Moreo, E. Dagotto, T. Jolicoeur, and J. Riera, *Phys. Rev. B* 42, 6283 (1990).
- [34] R. Hayn, A. F. Barabanov and J. Schulenburg, *Z. Phys. B* 102, 359 (1997).
- [35] A. F. Barabanov, V. M. Beresovsky, E. Zaslas, R. O. Kuzian, and L. A. Maksimov, *Zh. Eksp. Teor. Fiz.* 110, 1480 (1996); [*JETP* 83, 819 (1996)]; *J. Phys. Cond. Matter* 3, 9129 (1991); *Physica C* 252, 308 (1995); *Physica C* 212, 375 (1993).

- [36] Y. Sibata, T. Tohyama and S. Maekawa, Phys. Rev. B 59, 1840 (1999).
- [37] A. F. Barabanov, A. A. Kovalev, O. V. Urazhev, A. M. Belenouk, Phys. Lett. A 265, 221 (2000); Doklady Phys. 44, 188 (1999); Pis'ma Zh. Eksp. Teor. Fiz. 68, 386 (1998); JETP Lett. 68, 412 (1998).
- [38] J. Zaanen and A. M. Ole's, Phys. Rev. B 37, 9423 (1988).
- [39] M. S. Hybertsen, M. Schluter and N. E. Christensen, Phys. Rev. B 39, 9028 (1989).
- [40] K. T. Park, K. Terakura, T. Oguchi, A. Yanase and M. Ikeda, J. Phys. Soc. Jpn. 57, 3445 (1988).
- [41] A. K. McMahan, R. M. Martin and S. Satpathy, Phys. Rev. B 38, 6650 (1988).
- [42] J. R. Schrieffer, J. Low Temp. Phys. 99, 397 (1995).
- [43] A. F. Barabanov, E. Zasinskas, O. V. Urazhev and L. A. Maksimov, Pis'ma v Zh. Eksp. Teor. Fiz. 66, 173 (1997); JETP Lett. 66, 182 (1997).
- [44] R. O. Kuzian, R. Hayn, A. F. Barabanov, L. A. Maksimov, Phys. Rev. B 58, 6194 (1998).
- [45] A. F. Barabanov and V. M. Beresovsky, Zh. Eksp. Teor. Fiz. 106, 1156 (1994); JETP 79, 627 (1994); J. Phys. Soc. Jpn. 63, 3974 (1994); Phys. Lett. A 186, 175 (1994).
- [46] H. Shimahara, J. Phys. Soc. Jpn. 62, 1317 (1993).
- [47] Y. Takahashi, Z. Phys. B 71, 425 (1988).
- [48] M. S. Golden, V. Borisenko, S. Legner, et al., Adv. in Sol. St. Phys. (2000), in press.
- [49] S. Lenger, V. Borisenko, C. Durr, et al., Phys. Rev. B, (2000), in press.
- [50] V. G. Grigoryan, G. Paasch and S. L. Drechsler, Phys. Rev. B 60, 1340 (1999).